Eukaryotic initiation factor 5B (eIF5B) regulates temozolomide-mediated apoptosis in brain tumor stem cells (BTSCs).

Authors and Affiliations: Joseph A. Ross[1], Bo Young Ahn[3], Jennifer King[3], Kamiko R. Bressler[1]. Donna L. Senger[3,4,5], Nehal Thakor[1, 2, 3*]

[1] Alberta RNA Research and Training Institute (ARRTI), Department of Chemistry and Biochemistry, University of Lethbridge, Lethbridge, Alberta, Canada.

[2] Canadian Centre for Behavioral Neuroscience (CCBN), Department of Neuroscience, University of Lethbridge, Lethbridge, Alberta, Canada.

[3] Arnie Charbonneau Cancer Institute, Cumming School of Medicine, University of Calgary, Calgary, Alberta, Canada.

[4] Clark H. Smith Brain Tumour Centre, University of Calgary, Calgary, Alberta, Canada.

[5] Department of Oncology, University of Calgary, Calgary, Alberta, Canada.

Author Contributions: Joseph Ross: Conception and design, collection and assembly of data, data analysis and interpretation, manuscript writing. Bo Young Ahn and Jennifer King: Provision of expertise and protocols for working with BTSCs. Kamiko Bressler: Collection and assembly of data, manuscript editing. Donna Senger: Conception, Provision of study materials. Nehal Thakor: Conception and design, financial support, final approval of the manuscript.

***Corresponding Author:** Nehal Thakor, Ph.D., University of Lethbridge, 4401 University Drive W, Lethbridge, Alberta, T1K 3M4, Canada, Phone: 403-317-5055, Email: nthakor@uleth.ca

Abstract

Glioblastoma multiforme (GBM) is among the deadliest cancers, owing in part to complex inter- and intra-tumor heterogeneity and the presence of a population of stem-like cells called brain tumor stem cells (BTSCs/BTICs). These cancer stem cells survive treatment and confer resistance to the current therapies—namely, radiation and the chemotherapeutic, temozolomide (TMZ). TMZ induces cell death by alkylating DNA, and BTSCs resist this mechanism via a robust DNA damage response. Hence, recent studies aimed to sensitize BTSCs to TMZ using combination therapy, such as inhibition of DNA repair machinery. We have previously demonstrated in established GBM cell lines that eukaryotic initiation factor 5B (eIF5B) promotes the translation of pro-survival and anti-apoptotic proteins. Consequently, silencing eIF5B sensitizes these cells to TRAIL-induced apoptosis. However, established cell lines do not always recapitulate the features of human glioma. Therefore, we investigated this mechanism in patient-derived BTSCs. We show that silencing eIF5B leads to increased TMZ sensitivity in two BTSC lines, BT25 and BT48. Depletion of eIF5B decreases levels of anti-apoptotic proteins in BT48 and sensitizes these cells to TMZ-induced activation of caspase-3, cleavage of PARP, and apoptosis. We suggest that eIF5B represents a rational target to sensitize GBM tumors to the current standard-of-care.

Keywords: Eukaryotic initiation factor 5B (eIF5B), Brain tumor stem cells (BTSCs), Apoptosis, Temozolomide (TMZ), Glioblastoma multiforme (GBM)

Introduction

Glioblastoma multiforme (GBM) is the most lethal form of brain tumour in adults, with a median survival of just 15 months (Stupp et al. 2005). Several factors—including complex tumour heterogeneity and a sub-population of stem-like glioma cells, termed brain tumour stem cells (BTSCs) (Cusulin et al. 2015; Kelly et al. 2009)—promote resistance to conventional therapies, including radiotherapy and the standard-of-care chemotherapeutic agent temozolomide (TMZ) (Bao et al. 2006; Salmaggi et al. 2006). TMZ is an alkylating agent that produces toxic methyl adducts at O6-guanine, leading to activation of the mismatch repair pathway and ultimately, lethal DNA breaks (Mojas et al. 2007). Intrinsic TMZ resistance is primarily mediated by O6-methylguanine-DNA methyltransferase (MGMT), which removes the methyl adducts from the DNA (Kitange et al. 2009). Other mechanisms for resistance to alkylating agents include base-excision repair and homologous recombination (Gil Del Alcazar et al. 2016; Trivedi et al. 2005). In preclinical studies, combination therapy has been shown to improve the efficacy of TMZ by overcoming these resistance mechanisms (Lun et al. 2016; Yuan et al. 2018).

We have previously shown that in established GBM cell lines, eIF5B is required for optimal translation of anti-apoptotic and pro-survival proteins from internal ribosome entry site (IRES)-encoding mRNAs, including X-linked inhibitor of apoptosis (XIAP), B-cell lymphoma extra-large (Bcl-xL), cellular inhibitor of apoptosis protein 1 (cIAP1), and the short isoform of cellular FLICE-like inhibitory protein (c-FLIPs) (Ross et al. 2019). Consequently, depletion of eIF5B by RNAi sensitizes these cells to TNF-related apoptosis-inducing ligand (TRAIL), enhancing apoptosis by a caspase-8/9-dependent pathway (Ross et al. 2019). As both extrinsic (i.e. receptor mediated) and intrinsic (i.e. DNA damage-mediated) apoptotic pathways converge on caspases-9, we reasoned that eIF5B depletion would also sensitize GBM cells to TMZ. As

established cell lines do not always recapitulate the features of human glioma, we investigated this mechanism in patient-derived BTSCs. We show here that siRNA-mediated depletion of eIF5B sensitizes two BTSC lines, BT25 and BT48, to TMZ. We show in BT48 cells that silencing eIF5B leads to enhanced TMZ-mediated activation of caspase-3, cleavage of PARP, and apoptosis. Moreover, eIF5B depletion in these cells leads to modestly decreased levels of XIAP and cIAP1, and substantially decreased levels of Bcl-xL and c-FLIPs proteins. We suggest that eIF5B represents a novel target to sensitize BTSCs to temozolomide.

Materials and Methods

Cell culture, transfection, and reagents

BT48 (previously called 48EF) and BT25 (previously called 25M) have been previously described (Sarkar et al. 2014). Cells were cultured in serum-free media supplemented with epidermal growth factor, fibroblast growth factor, and heparan sulphate in a humidified incubator (37ºC, 5% CO_2) as described elsewhere (Kelly et al. 2009). To propagate these cells in monolayer, cells were dissociated with Accutase (Innovative Cell Technologies, San Diego, USA) and seeded into plates coated with laminin (Millipore Sigma, Toronto, Canada) at 1 μg/cm^2. U343 cells were propagated in Dulbecco's high modified Eagle's medium (DMEM, HyClone, Logan, USA) with 4 mM L-glutamine, 4500 mg/L glucose, and 1 mM sodium pyruvate supplemented with 10% fetal bovine serum (Gibco, Waltham, USA) and 1% penicillin-streptomycin (Gibco). Transfections were carried out using Opti-MEM (Gibco) and Lipofectamine RNAiMAX (Invitrogen, Madison, USA) according to manufacturer's instructions. Non-specific control siRNA and siRNAs targeting

eIF5B (HSS114469/70/71) were obtained from Qiagen (Hilden, Germany) and Invitrogen, respectively. TMZ was obtained from Active Biochem Ltd (Hong Kong, China).

Immunoblotting

Cells were seeded at 400,000 cells/well in 6-well plates, incubated 24 hours, and forward transfected. After a further 24 hours, TMZ or DMSO (vehicle control) were added where indicated. After a final 72 hours, cells were harvested, and immunoblotting was performed as previously described (Ross et al. 2019).

In vitro viability assay

Cells were seeded at 13,000 cells/well in 96-well plates, incubated 24 hours, and forward transfected. After a further 24 hours, cells were treated with a vehicle control (DMSO) or TMZ. Where indicated, cells were pre-treated for 2 hours with z-VAD-fmk (R & D Systems, Minneapolis, USA) or Necrostatin-1 (Millipore-Sigma) before adding TMZ. After a further 96 hours, cell viability was determined by alamarBlue assay (resazurin sodium salt; Sigma-Aldrich, Oakville, Canada) as previously described(Ross et al. 2019).

Microscopy

Cells were grown and treated the same as immunoblotting, except that instead of harvesting, a general DNA stain (1 µg/mL Hoechst 33342; Thermo Scientific, Waltham, USA) was added to the cells. After a 30-minute incubation, the cells were imaged in a Cytation 5 plate imager (BioTek, Winooski, USA). For fluorescence microscopy, cells were imaged using a DAPI filter to analyze

Hoechst-stained nuclear DNA. The percent of Hoechst-stained nuclei per field-of-view demonstrating fragmentation were quantified using the onboard Cytation 5 analysis software.

Statistical analyses

All quantitative data represent the mean ± standard error on the mean (SEM) for at least 3 independent biological replicates. Statistical significance was determined by an unpaired, two-tailed t-test. The significance level was set at a p-value of 0.05. Data were analyzed using GraphPad Prism, version 8.

Bioinformatics analyses

Kaplan-Meier survival curves were plotted using PROGgeneV2-Prognostic database (http://watson.compbio.iupui.edu/chirayu/proggene/database/?url=proggene) (Goswami and Nakshatri 2014). *EIF5B* mRNA levels across 20 cancer types were examined in The Cancer Genome Atlas (TCGA) cBioportal (http://www.cbioportal.org/) (Cerami et al. 2012).

Results

Depletion of eIF5B enhances TMZ-induced apoptosis in BTSCs.

We have previously demonstrated that depletion of eIF5B leads to increased apoptosis in GBM cell lines (Ross et al. 2019). However, established cell lines do not always recapitulate the features of human glioma. We therefore tested whether eIF5B depletion has a similar effect in BTSC cell lines (BT48 and BT25), which normally grow as neurospheres in liquid suspension (Figure 1A).

In order to deplete eIF5B by RNAi, we grew BT48 or BT25 cells in a monolayer on laminin-coated plates as previously described (Pollard et al. 2009), before transfecting with a non-specific control siRNA or a pool of eIF5B-specific siRNAs. We successfully depleted levels of the eIF5B protein by ~90% in both cell lines, leading to no significant effect on alamarBlue activity (Figure 1B). We next tested whether eIF5B depletion increases the sensitivity of BTSCs to a frontline therapeutic agent, TMZ. We measured the effects of various concentrations of TMZ on control or eIF5B-depleted BT25 or BT48 cells by alamarBlue assay. Indeed, silencing eIF5B decreased the IC_{50} of TMZ approximately 3- and 2-fold in BT25 and BT48, respectively (Figure 1C, D). Moreover, pre-treatment of the cells with a pan-caspase inhibitor (z-VAD-fmk) prevented the enhancement of TMZ sensitivity by eIF5B depletion, consistent with apoptotic cell death; conversely, the TMZ sensitivity phenotype was not reversed by a RIP1-kinase inhibitor (Necrostatin-1), indicating that eIF5B does not affect the ability of TMZ to induce necroptosis (Figure 1E).

To confirm that decreased alamarBlue activity is due to increased apoptosis, we performed a series of microscopy experiments in BT48. First, brightfield microscopy confirmed that TMZ-treated, eIF5B-silenced BT48 cells grew to a lower density compared to untreated control cells (Figure 2A, left panels). Moreover, the combination of eIF5B depletion and TMZ treatment led to an altered cell morphology (Figure 2A, left panels). Specifically, a large proportion of the cells shrank and became rounded, as opposed to the elongated adherent cells observed for untreated control cells. Consistent with apoptotic cell death, Hoechst live-cell nuclear staining revealed increased nuclear fragmentation and condensation in TMZ-treated, eIF5B-depleted cells (Figure 2A, middle and right panels, and Figure 2B). Finally, we observed a significant increase in cleaved caspase-3 and cleaved PARP in eIF5B-depleted, TMZ-treated cells (Figure 2C-F). Moreover,

depletion of eIF5B did not lead to decreased levels of the stemness marker, SRY-box 2 (SOX2), indicating that stemness was maintained in BT48 upon silencing eIF5B (Figure 2C). Taken together, the data indicate that depletion of eIF5B enhances sensitivity of BT48 cells to TMZ-induced apoptosis.

Depletion of eIF5B leads to reduced levels of anti-apoptotic proteins in BTSCs.

We have previously demonstrated that depletion of eIF5B leads to decreased translation of anti-apoptotic proteins in GBM cell lines (Ross et al. 2019). We therefore tested whether silencing eIF5B decreases the expression of such proteins in BT48 cells. Indeed, depletion of eIF5B lead to a modest but significant reduction in the levels of XIAP, cIAP1, and c-FLIP$_L$, and a more robust reduction (~2-fold) in Bcl-xL and c-FLIP$_S$ levels (Figure 3). This indicates that, consistent with our previous findings, eIF5B is important for the optimal expression of anti-apoptotic proteins.

Discussion

We show in this work that eIF5B depletion leads to decreased anti-apoptotic protein expression and increased TMZ sensitivity in BT48 BTSCs. Our findings are consistent with a recent body of work suggesting that eIF5B is involved in regulating pro-growth pathways (Jiang et al. 2016), central carbon metabolism and hypoxia adaptation of glioblastoma (Ho et al. 2018), and non-canonical translation by IRES- and uORF-mediated mechanisms (Joseph A. Ross 2018; Ross et al. 2019; Thakor and Holcik 2012).

Notably, the effects of eIF5B depletion on Bcl-xL and c-FLIP$_S$ levels were larger in magnitude than those observed for XIAP, cIAP1 and c-FLIP$_L$ (Figure 3). It is not surprising that

183 c-FLIP$_L$ levels decreased modestly upon eIF5B depletion, as we previously observed a similar
184 phenotype in an established GBM cell line (U343) which we attributed to the lack of an IRES
185 element in c-FLIP$_L$ (Ross et al. 2019). XIAP is translated from two alternative transcripts, only
186 one of which encodes an IRES; as we have previously demonstrated that eIF5B is important for
187 IRES-dependent translation of XIAP (Thakor and Holcik 2012), this could explain the relatively
188 modest drop in XIAP levels reported here. Members of the inhibitor of apoptosis protein (IAP)
189 family (e.g. XIAP, cIAP1) function as competitive inhibitors of caspases (Roy et al. 1997). XIAP,
190 the most potent of the IAPs, plays a key role in suppressing the activity of caspase-9 and the
191 executioner caspases (Silke and Meier 2013). Bcl-xL inhibits pore formation by Bim, Bid, Bax,
192 and Bak, which would otherwise cause mitochondrial outer membrane permeabilization (MOMP)
193 (Lomonosova and Chinnadurai 2008). c-FLIP is expressed in humans as a short isomer (c-FLIP$_S$)
194 and a long isomer (c-FLIP$_L$), both of which can inhibit caspase-8 activation by death receptors
195 (Safa 2013).

196 Depletion of eIF5B did not lead to decreased levels of SOX2, a transcription factor
197 essential for self-renewal or pluripotency (Figure 2C). The effect of eIF5B depletion on TMZ
198 sensitivity in BTSCs is therefore unlikely due to any loss of stemness. The robust levels of SOX2
199 detected here are in line with Pollard et al. (2009), who demonstrated that glioma stem cells
200 expanded in adherent culture on laminin-coated plates recapitulated the features of neural stem
201 cells—including the expression of stemness markers like SOX2 (Pollard et al. 2009).

202 Importantly, the increase in TMZ sensitivity upon eIF5B depletion was prevented by z-
203 VAD-fmk but not by Necrostatin-1, suggesting that eIF5B promotes resistance to caspase
204 activation (Figure 1E). This notion was supported by microscopy, which indicated increased
205 nuclear condensation and fragmentation—indicative of apoptotic cell death (Tsujimoto 2012)—in

TMZ-treated, eIF5B-depleted BT48 cells (Figure 2A). We also observed significantly increased caspase-3 activation and PARP cleavage upon eIF5B depletion (Figure 2C). Notably, we used an antibody specific for the 89 kDa C-terminal fragment of PARP classically generated by caspase-3 cleavage (Chaitanya et al. 2010). Cleavage of PARP by caspases separates its catalytic domain from its DNA-binding domain, attenuating DNA repair (Chaitanya et al. 2010). Interestingly, the PARP cleavage observed here did not depend entirely upon TMZ treatment, as eIF5B depletion also enhanced PARP cleavage in the absence of TMZ (Figure 2C). This suggests that eIF5B protects PARP from cleavage resulting from a pro-apoptotic stimulus besides TMZ. We previously demonstrated that eIF5B depletion leads to decreased levels of the master regulator of oxidative stress response, NRF2, leading to increased ROS accumulation in an established GBM cell line (Ross et al. 2019). It is possible that eIF5B depletion has a similar effect in BT48. Increased oxidative stress would cause increased MOMP and, hence, increased caspase activation (Sinha et al. 2013), which would be further enhanced by decreased levels of Bcl-xL and other anti-apoptotic proteins. Thus, we propose that eIF5B depletion sensitizes BT48 cells to intrinsic apoptosis stimulated by TMZ-induced DNA damage due to decreased levels of anti-apoptotic proteins. Moreover, the increased cleavage of PARP would lead to a less robust repair response to the DNA damage caused by TMZ.

Transcript levels are routinely measured from tumors and are corelated with patient survival. In line with this notion, using The Cancer Genome Atlas (TCGA) data, Yi et al. (2018) correlated decreased levels of *EIF5B* mRNA with worse outcome for patients with glioblastoma (Yi et al. 2018). eIF5B at the protein level does not work alone, and its dynamic interactions with eIF1A, eIF2A, and eIF5 play a critical role in regulating non-canonical translation (Kim et al. 2018; Lin et al. 2018; Nag et al. 2016). For example, eIF5B interacts with eIF1A to stabilize

initiator tRNA into the ribosome (Lin et al. 2018; Nag et al. 2016). Its interaction with eIF5 regulates the displacement of initiator tRNA from ternary complex (eIF2-GTP-Met-tRNAi). However, eIF1A and eIF5 have conserved eIF5B-binding sequences and they compete to bind to eIF5B (Lin et al. 2018). Moreover, eIF2A (not to confuse with eIF2α) binds and cooperates with eIF5B to deliver initiator tRNA to the ribosome, specifically during IRES-mediated translation initiation (Kim et al. 2018). We have demonstrated that the stoichiometry between eIF5B and its interacting partner(s) is critical for uORF-mediated non-canonical translation initiation (Joseph A. Ross 2018). These findings suggest that eIF5B is a critical scaffolding protein for regulating non-canonical translation initiation via its dynamic interactions with eIF1A, eIF2A, and eIF5. Therefore, *EIF5B* mRNA levels alone should not be used as a prognostic marker for GBM patient survival. To this end, we have looked at the association between ratios of *EIF5B/EIF2A*, *EIF5B/EIF1AX*, and *EIF5B/EIF5* mRNAs and overall survival of GBM patients using various patient cohorts (Supplemental Figure S1). These data suggest that higher levels of *EIF5B* mRNA over *EIF1AX, EIF2A*, and *EIF5* was correlated with worse patient outcomes. Further, Yi et al. (2018) also showed that eIF5B levels decrease in TMZ-treated U87 cells. Moreover, our data suggest that *EIF5B* is not lost in GBM (Supplemental Figure S2), in fact, eIF5B protein levels are modestly enhanced in TMZ-treated U343 cells and brain tumor initiating cells (BTICs) (Supplemental Figure S3 and Figure 2D, respectively). Additionally, the ratios of eIF5B/eIF1A, eIF5B/eIF5, and eIF5B/eIF2A proteins are also modestly enhanced (Supplemental Figure S3) under TMZ treatment in U343 cells. It is known that TMZ-mediated genotoxic stress induces the production of reactive oxygen species (ROS) (Jiang et al. 2012; Lee et al. 2014) that leads to eIF2α phosphorylation (Supplemental Figure S3). TMZ enhances the unfolded protein response (UPR) in GBM cells (Jiang et al. 2012; Lee et al. 2014; Yuan et al. 2012; Zeeshan et al. 2016). Under this

condition canonical translation would be attenuated due to eIF2α phosphorylation. However, the enhanced levels of eIF5B would execute the switch from canonical to non-canonical translation and would likely support the cell survival by facilitating non-canonical translation XIAP, Bcl-xL, cIAP1, and cFLIPs. Interestingly, eIF5B depletion leads to downregulation of these anti-apoptotic proteins and sensitizes GBM cells to pro-apoptotic agents. Therefore, in contrast to Yi. G. Z., et al. (2018), our data warrants a study on validating eIF5B as a therapeutic target for GBM tumors.

Acknowledgments: This work was funded by the Canada Foundation for Innovation-John R. Evans Leaders Fund (35017), the Rare Disease Foundation and BC Children's Hospital Foundation (17-39), the Campus Alberta Innovates Program, Alberta Innovates Health Solutions, and the Alberta Ministry of Economic Development and Trade.

Conflict of Interest

The authors declare no competing interests.

References

Bao, S., Wu, Q., McLendon, R.E., Hao, Y., Shi, Q., Hjelmeland, A.B., et al. 2006. Glioma stem cells promote radioresistance by preferential activation of the DNA damage response. Nature **444**(7120): 756-760. doi:10.1038/nature05236.

Cerami, E., Gao, J., Dogrusoz, U., Gross, B.E., Sumer, S.O., Aksoy, B.A., et al. 2012. The cBio cancer genomics portal: an open platform for exploring multidimensional cancer genomics data. Cancer Discov **2**(5): 401-404. doi:10.1158/2159-8290.CD-12-0095.

Chaitanya, G.V., Steven, A.J., and Babu, P.P. 2010. PARP-1 cleavage fragments: signatures of cell-death proteases in neurodegeneration. Cell communication and signaling : CCS **8**: 31. doi:10.1186/1478-811x-8-31.

Cusulin, C., Chesnelong, C., Bose, P., Bilenky, M., Kopciuk, K., Chan, J.A., et al. 2015. Precursor States of Brain Tumor Initiating Cell Lines Are Predictive of Survival in Xenografts and Associated with Glioblastoma Subtypes. Stem cell reports **5**(1): 1-9. doi:10.1016/j.stemcr.2015.05.010.

Gil Del Alcazar, C.R., Todorova, P.K., Habib, A.A., Mukherjee, B., and Burma, S. 2016. Augmented HR Repair Mediates Acquired Temozolomide Resistance in Glioblastoma. Molecular cancer research : MCR **14**(10): 928-940. doi:10.1158/1541-7786.mcr-16-0125.

Goswami, C.P., and Nakshatri, H. 2014. PROGgeneV2: enhancements on the existing database. BMC Cancer **14**: 970. doi:10.1186/1471-2407-14-970.

Ho, J.J.D., Balukoff, N.C., Cervantes, G., Malcolm, P.D., Krieger, J.R., and Lee, S. 2018. Oxygen-Sensitive Remodeling of Central Carbon Metabolism by Archaic eIF5B. Cell reports **22**(1): 17-26. doi:10.1016/j.celrep.2017.12.031.

Jiang, X., Jiang, X., Feng, Y., Xu, R., Wang, Q., and Deng, H. 2016. Proteomic Analysis of eIF5B Silencing-Modulated Proteostasis. PLoS One **11**(12): e0168387. doi:10.1371/journal.pone.0168387.

Jiang, Y., Sun, Y., and Yuan, Y. 2012. [Mechanism of temozolomide-induced anti-tumor effects on glioblastoma cells in vitro is via ROS-dependent SIRT1 signaling pathway]. Zhonghua Zhong Liu Za Zhi **34**(10): 734-738. doi:10.3760/cma.j.issn.0253-3766.2012.10.004.

Joseph A. Ross, K.R.B., Nehal Thakor. 2018. Eukaryotic Initiation Factor 5B (eIF5B) Cooperates with eIF1A and eIF5 to Facilitate uORF2-Mediated Repression of ATF4 Translation. International Journal of Molecular Sciences **19**(12): 4032.

Kelly, J.J., Stechishin, O., Chojnacki, A., Lun, X., Sun, B., Senger, D.L., et al. 2009. Proliferation of human glioblastoma stem cells occurs independently of exogenous mitogens. Stem Cells **27**(8): 1722-1733. doi:10.1002/stem.98.

Kim, E., Kim, J.H., Seo, K., Hong, K.Y., An, S.W.A., Kwon, J., et al. 2018. eIF2A, an initiator tRNA carrier refractory to eIF2alpha kinases, functions synergistically with eIF5B. Cell Mol Life Sci **75**(23): 4287-4300. doi:10.1007/s00018-018-2870-4.

Kitange, G.J., Carlson, B.L., Schroeder, M.A., Grogan, P.T., Lamont, J.D., Decker, P.A., et al. 2009. Induction of MGMT expression is associated with temozolomide resistance in glioblastoma xenografts. Neuro-oncology **11**(3): 281-291. doi:10.1215/15228517-2008-090.

Lee, S., Truesdell, S.S., Bukhari, S.I., Lee, J.H., LeTonqueze, O., and Vasudevan, S. 2014. Upregulation of eIF5B controls cell-cycle arrest and specific developmental stages. Proc Natl Acad Sci U S A **111**(41): E4315-4322. doi:10.1073/pnas.1320477111.

Lin, K.Y., Nag, N., Pestova, T.V., and Marintchev, A. 2018. Human eIF5 and eIF1A Compete for Binding to eIF5B. Biochemistry **57**(40): 5910-5920. doi:10.1021/acs.biochem.8b00839.

Lomonosova, E., and Chinnadurai, G. 2008. BH3-only proteins in apoptosis and beyond: an overview. Oncogene **27 Suppl 1**: S2-19. doi:10.1038/onc.2009.39.

Lun, X., Wells, J.C., Grinshtein, N., King, J.C., Hao, X., Dang, N.H., et al. 2016. Disulfiram when Combined with Copper Enhances the Therapeutic Effects of Temozolomide for the Treatment of Glioblastoma. Clinical cancer research : an official journal of the American Association for Cancer Research **22**(15): 3860-3875. doi:10.1158/1078-0432.ccr-15-1798.

Mojas, N., Lopes, M., and Jiricny, J. 2007. Mismatch repair-dependent processing of methylation damage gives rise to persistent single-stranded gaps in newly replicated DNA. Genes & development **21**(24): 3342-3355. doi:10.1101/gad.455407.

Nag, N., Lin, K.Y., Edmonds, K.A., Yu, J., Nadkarni, D., Marintcheva, B., et al. 2016. eIF1A/eIF5B interaction network and its functions in translation initiation complex assembly and remodeling. Nucleic acids research **44**(15): 7441-7456. doi:10.1093/nar/gkw552.

Pollard, S.M., Yoshikawa, K., Clarke, I.D., Danovi, D., Stricker, S., Russell, R., et al. 2009. Glioma stem cell lines expanded in adherent culture have tumor-specific phenotypes and are suitable for chemical and genetic screens. Cell stem cell **4**(6): 568-580. doi:10.1016/j.stem.2009.03.014.

Ross, J.A., Dungen, K.V., Bressler, K.R., Fredriksen, M., Khandige Sharma, D., Balasingam, N., et al. 2019. Eukaryotic initiation factor 5B (eIF5B) provides a critical cell survival switch to glioblastoma cells via regulation of apoptosis. Cell Death Dis **10**(2): 57. doi:10.1038/s41419-018-1283-5.

Roy, N., Deveraux, Q.L., Takahashi, R., Salvesen, G.S., and Reed, J.C. 1997. The c-IAP-1 and c-IAP-2 proteins are direct inhibitors of specific caspases. The EMBO journal **16**(23): 6914-6925. doi:10.1093/emboj/16.23.6914.

Safa, A.R. 2013. Roles of c-FLIP in Apoptosis, Necroptosis, and Autophagy. J Carcinog Mutagen **Suppl 6**. doi:10.4172/2157-2518.S6-003.

Salmaggi, A., Boiardi, A., Gelati, M., Russo, A., Calatozzolo, C., Ciusani, E., et al. 2006. Glioblastoma-derived tumorospheres identify a population of tumor stem-like cells with angiogenic potential and enhanced multidrug resistance phenotype. Glia **54**(8): 850-860. doi:10.1002/glia.20414.

Sarkar, S., Doring, A., Zemp, F.J., Silva, C., Lun, X., Wang, X., et al. 2014. Therapeutic activation of macrophages and microglia to suppress brain tumor-initiating cells. Nat Neurosci **17**(1): 46-55. doi:10.1038/nn.3597.

Silke, J., and Meier, P. 2013. Inhibitor of apoptosis (IAP) proteins-modulators of cell death and inflammation. Cold Spring Harb Perspect Biol **5**(2). doi:10.1101/cshperspect.a008730.

Sinha, K., Das, J., Pal, P.B., and Sil, P.C. 2013. Oxidative stress: the mitochondria-dependent and mitochondria-independent pathways of apoptosis. Archives of toxicology **87**(7): 1157-1180. doi:10.1007/s00204-013-1034-4.

Stupp, R., Mason, W.P., van den Bent, M.J., Weller, M., Fisher, B., Taphoorn, M.J., et al. 2005. Radiotherapy plus concomitant and adjuvant temozolomide for glioblastoma. The New England journal of medicine **352**(10): 987-996. doi:10.1056/NEJMoa043330.

Thakor, N., and Holcik, M. 2012. IRES-mediated translation of cellular messenger RNA operates in eIF2alpha- independent manner during stress. Nucleic acids research **40**(2): 541-552. doi:10.1093/nar/gkr701.

Trivedi, R.N., Almeida, K.H., Fornsaglio, J.L., Schamus, S., and Sobol, R.W. 2005. The role of base excision repair in the sensitivity and resistance to temozolomide-mediated cell death. Cancer research **65**(14): 6394-6400. doi:10.1158/0008-5472.can-05-0715.

Tsujimoto, Y. 2012. Multiple ways to die: non-apoptotic forms of cell death. Acta oncologica (Stockholm, Sweden) **51**(3): 293-300. doi:10.3109/0284186x.2011.648340.

Yi, G.Z., Xiang, W., Feng, W.Y., Chen, Z.Y., Li, Y.M., Deng, S.Z., et al. 2018. Identification of Key Candidate Proteins and Pathways Associated with Temozolomide Resistance in Glioblastoma Based on Subcellular Proteomics and Bioinformatical Analysis. Biomed Res Int **2018**: 5238760. doi:10.1155/2018/5238760.

Yuan, A.L., Ricks, C.B., Bohm, A.K., Lun, X., Maxwell, L., Safdar, S., et al. 2018. ABT-888 restores sensitivity in temozolomide resistant glioma cells and xenografts. PloS one **13**(8): e0202860. doi:10.1371/journal.pone.0202860.

Yuan, Y., Xue, X., Guo, R.B., Sun, X.L., and Hu, G. 2012. Resveratrol enhances the antitumor effects of temozolomide in glioblastoma via ROS-dependent AMPK-TSC-mTOR signaling pathway. CNS Neurosci Ther **18**(7): 536-546. doi:10.1111/j.1755-5949.2012.00319.x.

Zeeshan, H.M., Lee, G.H., Kim, H.R., and Chae, H.J. 2016. Endoplasmic Reticulum Stress and Associated ROS. Int J Mol Sci **17**(3): 327. doi:10.3390/ijms17030327.

Figure Captions

Figure 1. Depletion of eIF5B sensitizes BTSCs to TMZ. (A) BT25 and BT48 neurospheres were grown for 1 week in liquid suspension and imaged at 10x magnification. **(B-D)** BT25 or BT48 cells were transfected with a non-specific control siRNA (siC) or an eIF5B-specific siRNA pool (si5B) and treated with a vehicle control (0.5% DMSO) or various concentrations of TMZ. AlamarBlue activity was measured after a further 96 hours. In (C) and (D), the resulting fluorescence readings are expressed as percent alamarBlue activity, where the readings for control or eIF5B-depleted cells were each normalized to the vehicle treatment. **(E)** Control or eIF5B-depleted BT48 cells were pre-treated with a vehicle control (0.5% DMSO), z-VAD-fmk (20 μM), or Necrostatin-1 (100 μM) for 2 hours before adding 62.5 μM TMZ or a further 0.5% DMSO (vehicle control). Data are expressed as mean ± SEM for three independent biological replicates. *, $p < 0.05$; **, $p < 0.01$.

Figure 2. Depletion of eIF5B enhances TMZ-induced apoptosis. (A) Control or eIF5B-depleted BT48 cells were treated with 62.5 μM TMZ or a vehicle control (0.5% DMSO) for 24 hours and stained with Hoechst 33342 for 30 minutes. The cells were then imaged at 20x magnification (left) by brightfield microscopy, or at 20x magnification (middle) and 40x magnification (right) by fluorescence microscopy to image DNA (blue). Images from a representative experiment are shown in the left and middle panels; images from a separate experiment are shown in the right

panels. **(B)** The percent of Hoechst-stained nuclei per field-of-view demonstrating fragmentation were quantified using the onboard Cytation 5 analysis software. The percent of Hoechst-stained nuclei from (A) displaying fragmentation (white arrows) were quantified. **(C-F)** Control or eIF5B-depleted BT48 cells were treated with 62.5 μM TMZ or a vehicle control (0.5% DMSO) for 72 hours, harvested in RIPA lysis buffer, and 30 μg of total protein resolved by SDS-PAGE before performing immunoblotting. **(C)** Representative immunoblots probing for eIF5B, caspase-3 (Pro-Cas-3), cleaved caspase-3 (Cas-3), cleaved PARP (Clv PARP), SOX2 (n=1), and β-actin (internal control). **(D-F)** Quantitation of eIF5B **(D)**, cleaved- versus pro-caspase-3 **(E)**, or cleaved PARP **(F)**, all normalized to β-actin. Data are expressed as mean ± SEM for three independent biological replicates. *, $p < 0.05$; **, $p < 0.01$; ***, $p < 0.001$; ****, $p < 0.0001$.

Figure 3. Depletion of eIF5B leads to decreased levels of anti-apoptotic proteins. Control or eIF5B-depleted cells were harvested in RIPA lysis buffer and 25 μg of total protein resolved by SDS-PAGE before performing immunoblotting. **(A)** Representative images of immunoblots probing for eIF5B, XIAP, cIAP1, Bcl-xL, c-FLIP$_L$, c-FLIP$_S$, or β-actin (internal control). **(B)** Quantitation of eIF5B, XIAP, cIAP1, Bcl-xL, c-FLIP$_L$, or c-FLIP$_S$, all normalized to β-actin. Data are expressed as mean ± SEM for three (cIAP1, c-FLIP$_S$, c-FLIP$_L$) and four (eIF5B, XIAP, Bcl-xL) independent biological replicates. *, $p < 0.05$; **, $p < 0.01$; ***, $p < 0.001$; ****, $p < 0.0001$.

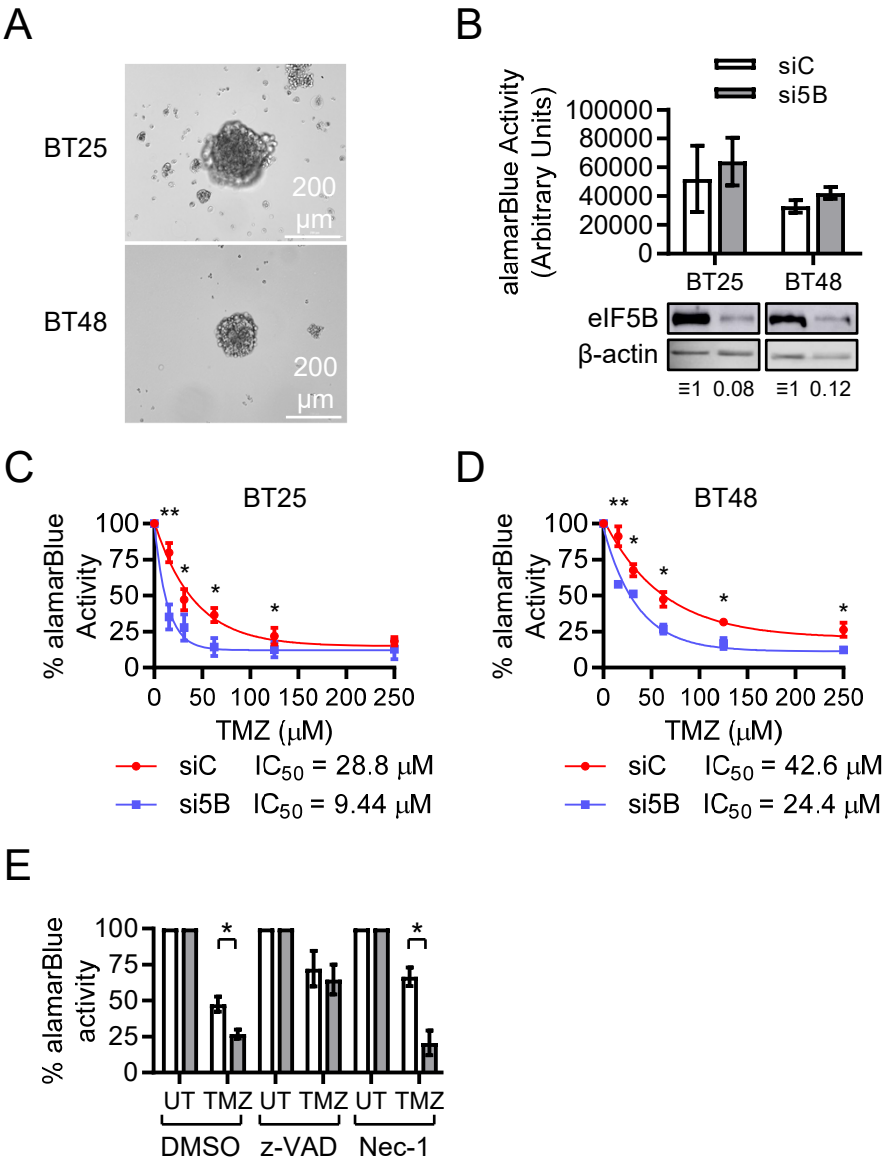
A
BT25
200 µm
BT48
200 µm
B
siC
si5B
alamarBlue Activity (Arbitrary Units)
100000
80000
60000
40000
20000
0
BT25
BT48
eIF5B
β-actin
≡1 0.08
≡1 0.12
C
BT25
% alamarBlue Activity
100
75
50
25
0
0 50 100 150 200 250
TMZ (µM)
siC IC50 = 28.8 µM
si5B IC50 = 9.44 µM
D
BT48
% alamarBlue Activity
TMZ (µM)
siC IC50 = 42.6 µM
si5B IC50 = 24.4 µM
E
% alamarBlue activity
UT TMZ UT TMZ UT TMZ
DMSO z-VAD Nec-1

Figure 1

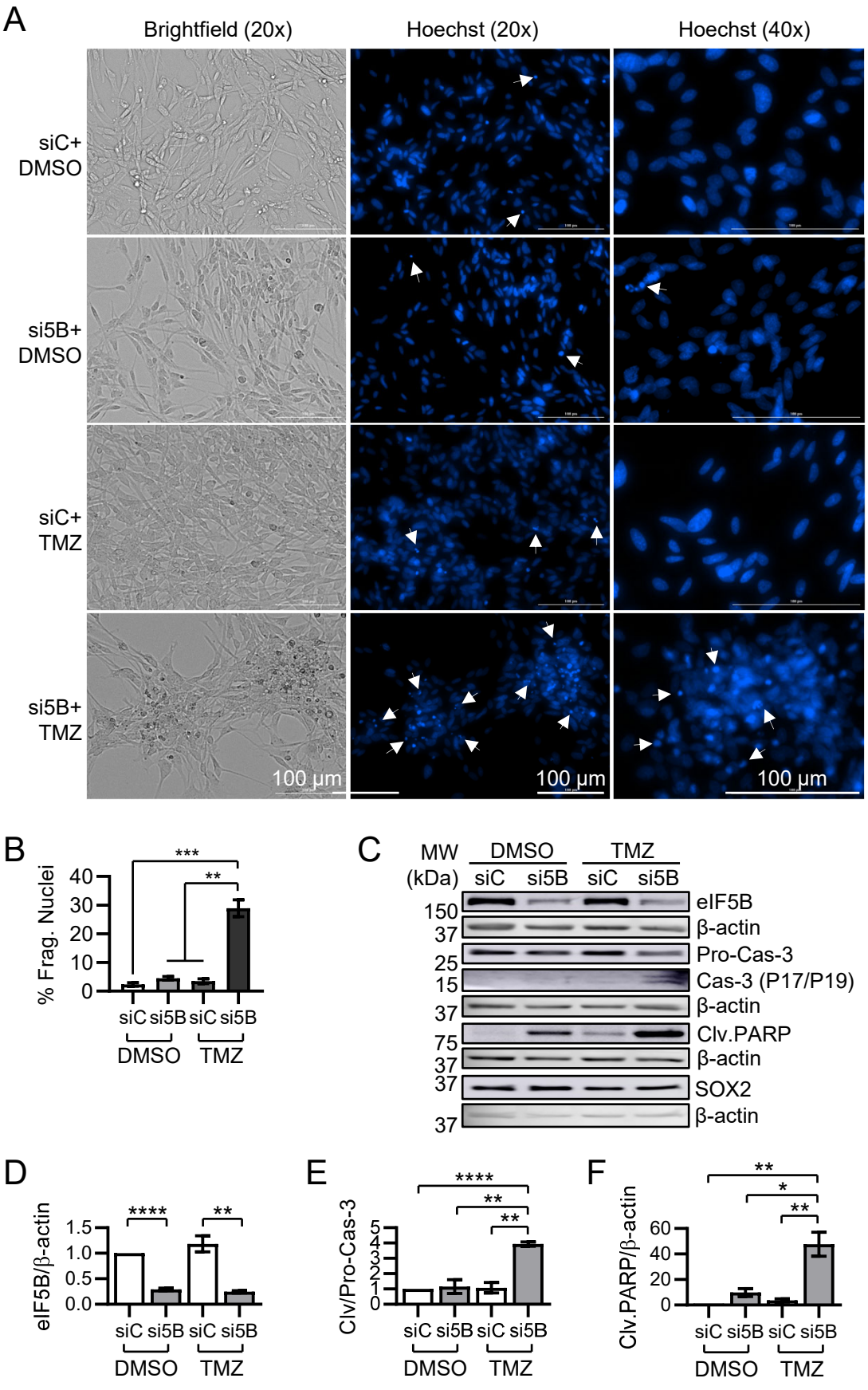
A
Brightfield (20x)
Hoechst (20x)
Hoechst (40x)
siC+ DMSO
si5B+ DMSO
siC+ TMZ
si5B+ TMZ
100 µm
100 µm
100 µm
B
% Frag. Nuclei
***
**
siC si5B siC si5B
DMSO TMZ
C
MW (kDa)
DMSO
TMZ
siC si5B siC si5B
150
37
25
15
37
75
37
37
37
eIF5B
β-actin
Pro-Cas-3
Cas-3 (P17/P19)
β-actin
Clv.PARP
β-actin
SOX2
β-actin
D
eIF5B/β-actin
****
**
siC si5B siC si5B
DMSO TMZ
E
Clv/Pro-Cas-3
****
**
**
siC si5B siC si5B
DMSO TMZ
F
Clv.PARP/β-actin
**
*
**
siC si5B siC si5B
DMSO TMZ

Figure 2

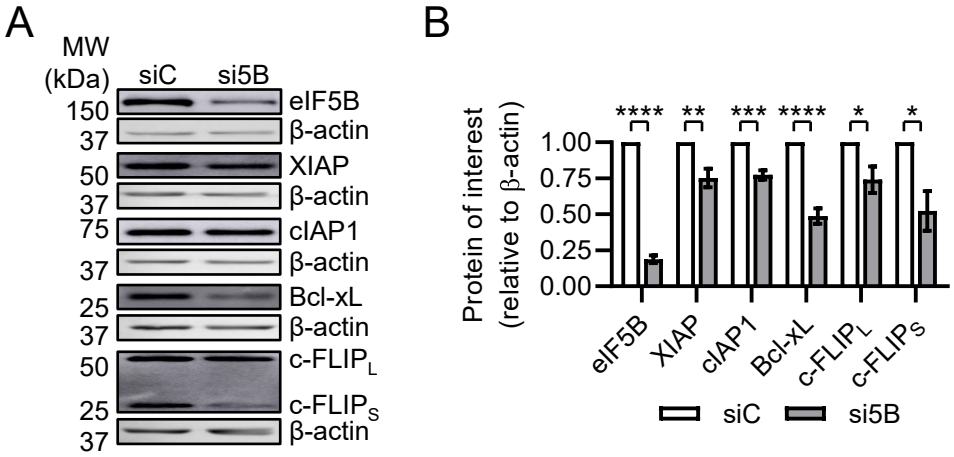
A
MW
(kDa)
siC
si5B
150
eIF5B
37
β-actin
50
XIAP
37
β-actin
75
cIAP1
37
β-actin
25
Bcl-xL
37
β-actin
50
c-FLIPL
25
c-FLIPS
37
β-actin
B
Protein of interest
(relative to β-actin)
1.00
0.75
0.50
0.25
0.00
****
**
***
****
*
*
eIF5B
XIAP
cIAP1
Bcl-xL
c-FLIPL
c-FLIPS
siC
si5B

Figure 3

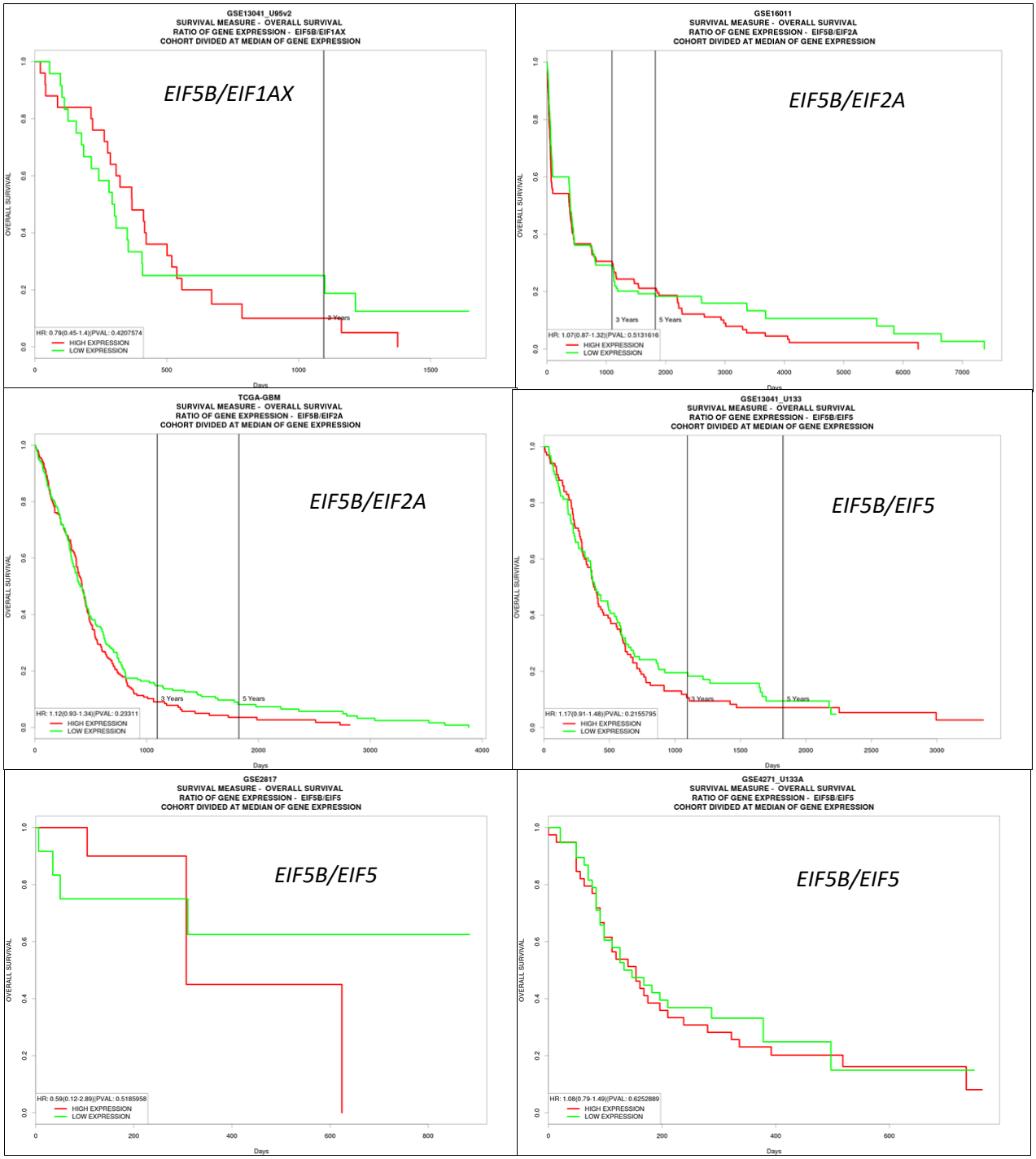

Supplemental Figure S1: We have looked at the association between ratios of *EIF5B/EIF2A*, *EIF5B/EIF1AX*, and *EIF5B/EIF5* mRNAs and overall survival of GBM patients using various patient cohorts. These data suggest that higher levels of *EIF5B* mRNA over *EIF1AX, EIF2A*, and *EIF5* were correlated with worse patient outcomes.

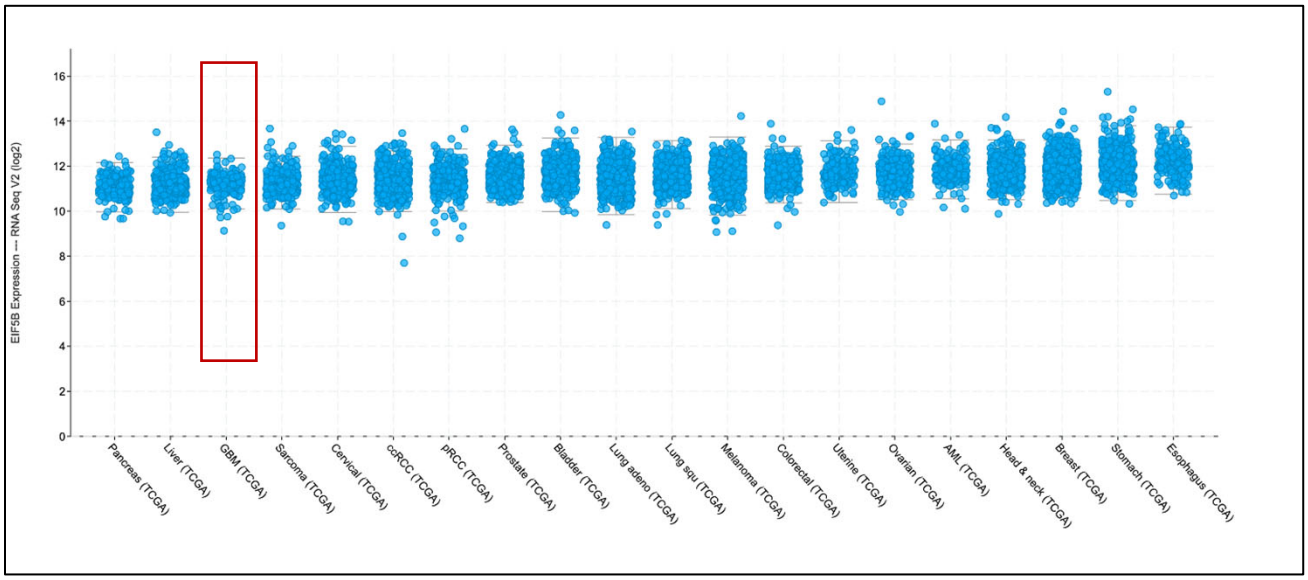

Supplemental Figure S2: Increasing median expression of EIF5B mRNA in various cancer types, suggesting that EIF5B is not lost in GBM.

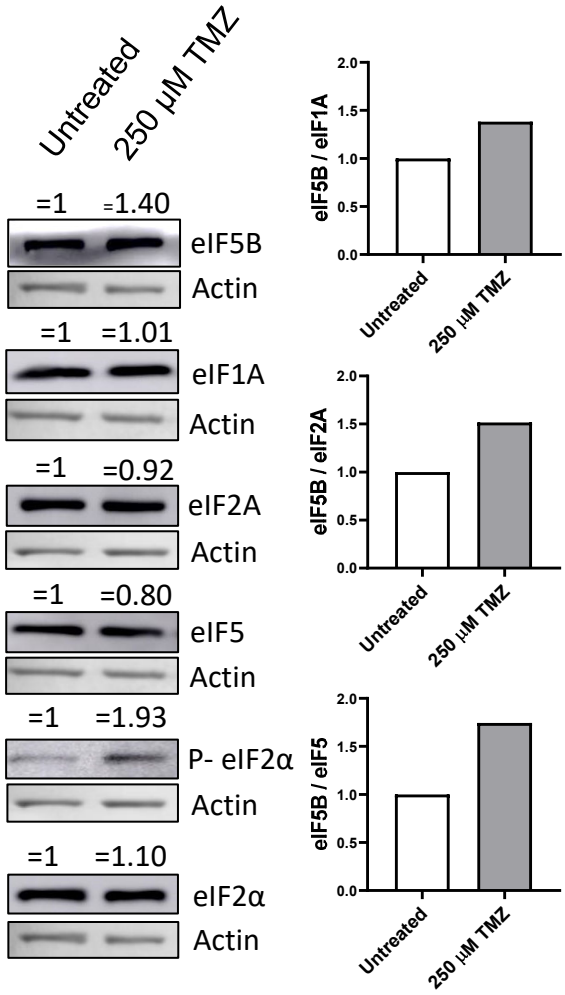

Supplemental Figure S3: The protein level of eIF5B modestly increases in TMZ-treated U343 cells. The ratios of eIF5B/eIF1A, eIF5B/eIF2A, and eIF5B/eIF5 are modestly enhanced upon TMZ treatment. U343 cells were treated with 250 μM TMZ for 24 hours, harvested in RIPA lysis buffer and 25 μg of total protein was resolved by SDS-PAGE before performing immunoblotting.